Astron. Astrophys. 279, L29–L32 (1993)

ASTRONOMY AND ASTROPHYSICS

Letter to the Editor

Evidence for siphon flows with shocks in solar magnetic flux tubes

D. Degenhardt[1], **S. K. Solanki**[2], **B. Montesinos**[3], **and J. H. Thomas**[4]

[1] Universitäts-Sternwarte, Geismarlandstrasse 11, D-37083 Göttingen, Germany
[2] Institute of Astronomy, ETH-Zentrum, CH-8092 Zürich, Switzerland
[3] LAEFF, ESA Villafranca Satellite Tracking Station, P.O. Box 50727, E-28080 Madrid, Spain
[4] Department of Mechanical Engineering, Department of Physics and Astronomy, and C. E. K. Mees Observatory, University of Rochester, Rochester, NY 14627, USA

Received 15 June 1993/Accepted 19 August 1993

Abstract. We synthesize profiles of the infrared line Fe I 15648.5 Å ($g = 3$) for a recently developed theoretical model of siphon flows along photospheric magnetic loops. The synthesized line profiles are compared with the observations from which Rüedi et al. (1992) deduced the presence of such flows across the neutral line of an active region plage. This comparison supports the interpretation of Rüedi et al. (1992). It also suggests that the average footpoint separation of the observed loops carrying the siphon flow is 8–15″ and that the siphon flow experiences a standing tube shock in the downstream leg near the top of the arch.

Key words: Sun: magnetic fields – Sun: active regions – magnetic flux tubes – siphon flows – radiative transfer

1. Introduction

In recent years considerable theoretical effort has been devoted to understanding the physics of siphon flows along magnetic flux tubes in the solar photosphere (Thomas 1988, Montesinos & Thomas 1989; 1993, Degenhardt 1989; 1991, Thomas & Montesinos 1990; 1991). Thomas (1988) suggested that siphon flows are a possible mechanism for producing some of the intense magnetic elements observed in the solar photosphere. Thomas & Montesinos (1991) gave the following description of the observational signature of a photospheric siphon flow:

"The observational signature of such a structure at the solar surface would be a pair of magnetic elements of opposite polarity, separated by a distance from one to several arcseconds, with slightly inclined magnetic fields and with an upflow in one element (the upstream footpoint of the arch) and a downflow and a somewhat greater magnetic field strength in the other element (the downstream footpoint)."

Recently, strong observational evidence for the existence of such siphon flows has been found by Rüedi et al. (1992), hereafter called RSR. They analysed Stokes V spectra of two infrared lines, Fe I 15648.5 Å ($g = 3$) and Fe I 15652.9 Å ($g_{\rm eff} = 1.53$), obtained in an active region plage with the entrance slit of the spectrograph placed across the neutral line. Their analysis of the line profiles at different spatial positions results in exactly the signature predicted for a siphon flow along a loop connecting magnetic elements across the neutral line.

In the present letter we describe synthetic line profiles of the 1.56μm line based upon detailed siphon flows calculated from theoretical models. A comparison with the observations then allows us to restrict the parameter range of the models. In particular, we find that even a qualitative comparison with the observations allows us to rule out purely subcritical flows without shocks in the downstream leg.

Send offprint requests to: D. Degenhardt

2. Magnetohydrodynamic models and diagnostic techniques

2.1. Siphon flows

The most highly developed models for steady siphon flows in thin, arched magnetic flux tubes include the radiative exchange of heat between the flux tube and its surroundings and calculate the paths of the tubes through the ambient medium self-consistently (Degenhardt 1991; Montesinos & Thomas 1993, hereafter called MT93). In addition, MT93 calculate critical siphon flows with adiabatic tube shocks in the downstream leg of the arch. As we shall see, a tube shock at some position in the downstream leg is necessary to reproduce the observations. Hence, except for test calculations with subcritical flows, all of the calculated siphon flows used in this paper are based on the formulation of MT93.

The essential features of the physical system (which are thoroughly documented by MT93) are as follows. The siphon flow is driven by a pressure difference between the two footpoints of the arch at the same gravitational potential. The flux tube arch is embedded in a nonmagnetic atmosphere which consists of model C of Vernazza et al. (1981) for the visible layers matched onto Spruit's (1974) model of the convection zone. Everywhere along the arch there is a transverse balance among the buoyancy force, the centrifugal force due to the siphon flow along the curved path, and the net magnetic tension force due to the curvature of the flux tube axis. For a subcritical siphon flow, the flow speed increases with height in

the upstream leg of the arch, reaches its maximum value at the top of the arch, and then decreases in the downstream leg. A critical siphon flow reaches the critical speed (the tube speed) somewhere near the top of the arch, continues to accelerate to supercritical speed, and then decelerates suddenly across a standing tube shock somewhere along the downstream leg of the arch, with the exact location of the shock depending on the pressure at the downstream footpoint.

2.2. Radiative transfer

We follow Degenhardt & Kneer (1992) and simplify the complicated geometry of a magnetic loop for the diagnostic radiative transfer by assuming that both legs of the arch are perpendicular to the solar surface. Then, the magnetic field strength $B(z)$ in the flux tube, its radius $R(z)$, the vertical component of the flow velocity $v_z(z)$, as well as the temperature $T(z)$ and density $\rho(z)$ both inside and outside the tubes are taken from the magnetohydrodynamic calculations. These simplifications are discussed in detail by Degenhardt & Kneer (1992).

We choose the infrared line, Fe I 15648.5Å ($g = 3$), the diagnostic capabilities of which are documented by Solanki et al. (1992). One of the properties of this line is its very deep level of formation. This is particularly useful, since the tubes are nearly vertical at these depths, so that the error introduced by 'rectifying' the legs of the magnetic arch is minimal. Next, assuming LTE and standard solar abundances, the hydrogen and electron densities, and thereby the continuum and line opacities, are calculated in all atmospheric components. Then, in the manner described by Kneer & von Uexküll (1991) we calculate the emergent Stokes I and V profiles for multiple equidistant rays parallel to the tube axis. The emergent profiles for each footpoint are then averaged with weights corresponding to the appertaining areas (1.5-D radiative transfer).

Before comparing synthetic with observed V profiles we must take into account the smearing due to seeing. If a, the e-folding width of the spatial smearing Gaussian $\exp -(x/a)^2$, is comparable to or larger than half the distance between the two footpoints, $2d$, then, in order to simulate the observed profile at a given spatial position x, we must superpose the suitably weighted profiles from the two footpoints. The weights are $\exp -(|d+x|/a)^2$ and $\exp -(|d-x|/a)^2$ for the footpoints at the positions $-d$ and d, respectively. In this way an additional parameter d/a is introduced.

3. Results

We have calculated several siphon flows with different initial conditions, resulting in both subcritical and critical flows in arches with various maximum heights. In Fig. 1 we display the Stokes I and V profiles emerging from the two legs of an arch with maximum height $z_{\max} = 478$ km (relative to $\tau = 1$ in the reference atmosphere) which contains a siphon flow. The initial conditions for the siphon-flow calculations, applied at the reference height $z = -200$ km, are as follows (the notation follows that of MT93): initial path angle $\theta_0 = 1.46$, tube radius $r_0 = 20$ km, flow speed $v_0 = 0.2385$ km/s, magnetic field strength $B_0 = 1797$ G ($\beta_0 = 2.5$), and temperature $T_0 = 10574$ K (equal to the exterior temperature at the same height). The siphon flow reaches the critical speed at the top of the arch. In the downstream leg the flow can either be subcritical or supercritical with a standing tube shock somewhere along the path of the tube. The run of the basic physical quantities with height for the subcritical flow and for flows with shocks in different locations is plotted by MT93.

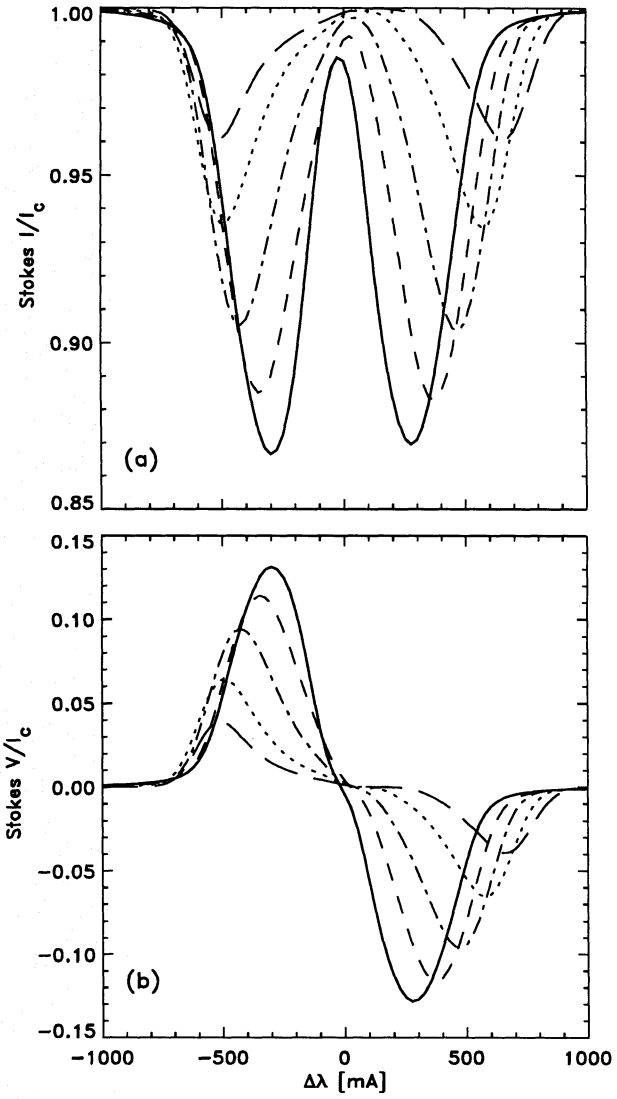

Fig. 1. (a) Synthetic Stokes I profiles (normalized to the continuum intensity) emerging from a set of siphon flow models. The solid line represents the profiles emerging from the upstream magnetic element, which is the same for all models. The other curves represent the downstream leg: subcritical downstream flow (dashed), shocked flows with shock positions at $z = 450$ km (dash–dotted), $z = 400$ km (dotted) and $z = 300$ km (long dashes). Note the strong increase of the line splitting with decreasing shock height. (b) Same as in (a) but for the Stokes V parameter. The polarity of the downstream profiles has been inverted for clarity.

As expected, the Stokes I profile and the zero–crossing of the Stokes V parameter in Fig. 1 show a weak blue shift for the upstream profile. Note the increase of both the line splitting and the redshift of the downstream profiles with decreasing height of the shock. This simply illustrates the basic features of shocked siphon flows. A lower shock location corresponds to a smaller internal gas pressure, and hence a stronger mag-

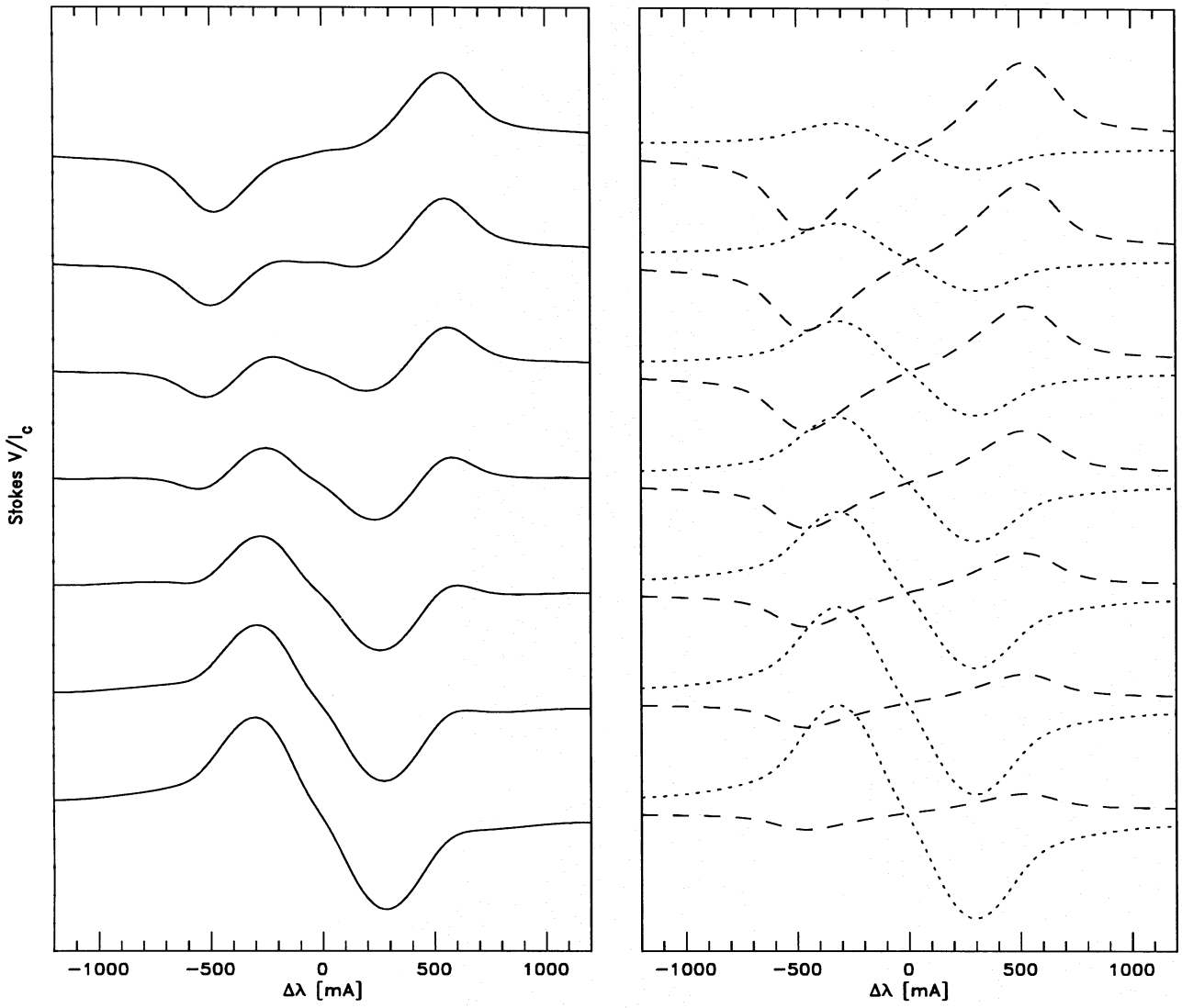

Fig. 2. Synthetic Stokes V profiles emerging from different spatial locations along a line which represents the entrance slit of a spectrograph placed across the neutral line of a plage region. The right panel shows the individual profiles contributing to the average profiles (left panel). This Figure should be compared with Fig. 2 of Rüedi et al. (1992).

netic field strength, at the downstream footpoint (see Fig. 2 in MT93).

The equivalent width of the downstream profiles decreases with decreasing height of the shock. This is due to the thermodynamic consequences of the siphon flow and the low height of formation of the infrared line. Due to the Wilson depression inside the flux tube, the line is formed below $\tau = 1$ of the reference atmosphere, in layers in which the radiative coupling between the flux tube and its surroundings is strong enough for the temperature of the tube to follow the external temperature. Hence, the temperature at $\tau_{1.6\mu} = 1$ inside the tube increases with decreasing shock height due to the increasing Wilson depression associated with the smaller internal gas pressure (see above). This results in a smaller equivalent width.

We now mix the individual line profiles in the manner described in Sect. 2.2 to model the effects of seeing and thus to simulate the observations of RSR. We assume that the two footpoints observed by RSR are connected by a loop. This is not a trivial assumption since, in the absence of the chromospheric and coronal vector field measurements, the connectivity of any two magnetic footpoints cannot be established. Nevertheless, the fact that the separation of the footpoints is similar to the spatial smearing due to seeing (see below) means that the field would have to be very strongly sheared or have a complex geometry in order to avoid a physical connection between the two observed footpoints.

The first result we find is that a subcritical flow fails to reproduce the observations. The reason has mainly to do with the difference in field strength between the upflow and downflow legs, as reflected in the splitting of the $g = 3$ line. Whereas the splitting difference is always smaller than 150 G for a subcritical flow, a difference of 300–400 G is required to reproduce the

data of RSR (the accuracy of the measured splitting is better than 100 G). A large number of test calculations using subcritical flows with different parameters confirms this result. Quite generally, subcritical flows are very nearly symmetric around the top of the arch, except for small differences introduced by the "hysterisis" produced by radiative transfer. Only a critical siphon flow with a shock in the downstream leg can produce the required splitting difference. We find that the best results are obtained for flows with a shock near the apex of the arch.

Figure 2 displays the results for a critical siphon flow with a shock at height $z = 430$ km, which is close to the top of the arch. Plotted are the "synthetic observations" at seven spatial positions, at locations (from bottom to top) $-0.6d$, $-0.4d$, $-0.2d$, 0, $0.2d$, $0.4d$, and $0.6d$, for a ratio $d/a = 0.8$, which implies that the individual footpoints cannot be completely resolved in the simulated observation. The magnetic field strength at the upstream footpoint has been adjusted so that the resulting Stokes V profile for the upstream magnetic element shows about the same Zeeman splitting as that inferred from the profiles measured by RSR. The right panel shows the individual profiles contributing to the averaged profiles plotted in the left panel. The dashed lines correspond to the profiles emerging from the downstream footpoint and the dotted lines represent the upstream profiles. All profiles have been spectrally convolved with a Gaussian having a Doppler width of approximately 6 km s^{-1} to account for instrumental smearing and macroturbulence (RSR).

The anomalously shaped profiles near the neutral line are similar to the profiles in Fig. 2 of RSR. The anomalous shapes of these profiles are due to the difference in the velocity shift and the Zeeman splitting of the two contributing profiles.

Finally, we find that in order to reproduce the observed line profiles for different spatial positions, d/a has to lie in the range 0.7–1.5. For values of d/a larger than 1.5 the individual profiles are clearly distinguishable with the result that the Stokes V profiles nearly vanish at the neutral line, in contrast to the observations. This and the comparison of the synthetic with the observed profiles suggest that the loops containing the siphon flows have a footpoint separation of 8–15″. It is also possible to model the observations by assuming each polarity to be composed of a number of footpoints located at different distances from the neutral line. However, this approach introduces an additional free parameter into the analysis, which, given the various underlying assumptions, appears unwarranted. We therefore restrict ourselves to a single loop and only note that if RSR see flows along multiple loops with different footpoint separations, we expect that the *average* footpoint separation is 8–15″.

4. Discussion and conclusions

We have shown that the Stokes V profiles observed by Rüedi et al. (1992) can be reproduced qualitatively by the theoretical siphon-flow model of Montesinos & Thomas (1993). In order to obtain a difference in the Zeeman splitting of the individual profiles emerging from the upstream and downstream magnetic elements that is large enough to reproduce the observed profiles, it is necessary to have a critical siphon flow with a standing tube shock in the downstream leg of the magnetic arch. For flux-tube arches reaching up to the temperature minimum, the location of the shock is close to the top of the arch. For shocks located further downstream the difference in Zeeman splitting between the Stokes V profiles of the two footpoints is too large and the line profile of the downstream element is too weak to contribute significantly to the average profile. Siphon flows along arches with lower maximum heights generally show the same effects, except that the shock has to be located further downstream.

Although the observations of RSR imply a shocked siphon flow, it is likely that subcritical siphon flows also exist on the sun, but these are more difficult to detect unambiguously due to the smaller differences between the upstream and downstream footpoints.

Finally, we stress the need for additional observations. Our conclusions suffer from two main uncertainties: 1. We cannot be certain that the two observed magnetic footpoints are really connected to each other. 2) It is unclear just how strongly the observed profiles are distorted by magneto-optical effects. These uncertainties can in future be substantially reduced by observing the full Stokes vector and by scanning the slit along the neutral line in order to get a two-dimensional magnetic and velocity map.

Acknowledgements. We are very grateful to Franz Kneer for many clarifying discussions and to an anonymous referee for helpful comments on the manuscript. This work has been supported in part by the Deutsche Forschungsgemeinschaft under grant DE177/10. J.H.T. was supported by NASA grants NAGW-2123 and NAGW-2444.

References

Degenhardt D., 1989, A&A 222, 297
Degenhardt D., 1991, A&A 248, 637
Degenhardt D., Kneer F., 1992, A&A 260, 411
Kneer F., von Uexküll M., 1991, A&A 247, 556
Montesinos B., Thomas J.H., 1989, ApJ 337, 977
Montesinos B., Thomas J.H., 1993, ApJ 402, 314
Rüedi I., Solanki S.K., Rabin D., 1992, A&A 261, L21
Solanki S.K., Rüedi I., Livingston W., 1992, A&A 263, 312
Spruit H.C., 1974, Solar Phys. 34, 277
Thomas J.H., 1988, ApJ 333, 407
Thomas J.H., Montesinos B., 1990, ApJ 359, 550
Thomas J.H., Montesinos B., 1991, ApJ 375, 404
Vernazza J.E., Avrett E.H., Loeser R., 1981, ApJS 45, 635

This article was processed by the author using Springer-Verlag TEX A&A macro package 1991.